FIRE PERFORMANCE OF AN UNPROTECTED COMPOSITE BEAM
Behavior with Finite Beam End Restraints, Rebar Size and Locations

Serdar Selamet [a]

[a] Bogazici University, Department of Civil Engineering, Bebek 34342 Istanbul, Turkey;
email: serdar.selamet@boun.edu.tr; tel: +90-212-359-6430

Abstract
The fire performance of steel connections is crucial to provide integrity and stability to floor systems. In full-scale fire tests, the steel frame systems experience large deflections and rotations, which in turn subject the connections to large axial forces and moments. The shear connections, which have limited rotational allowance due to a small gap distance between the beam and the supporting member, exhibit a semi-rigid behavior during fire. Further, the effect of the concrete slab is observed to be beneficial to the deflection behavior of the floor system in several experiments. In this study, the fire performance of a beam with a concrete slab is investigated with varying degrees of rotational rigidity and the tension capacity of the concrete slab with steel rebars. The thermo-mechanical analysis capability of Opensees is utilized.

Keywords: steel beam, composite beam, connection, restraints, Cardington, fire, Opensees

INTRODUCTION

A recent capability in analyzing the thermo-mechanical problems is added to Opensees by the research team in University of Edinburgh in U.K, which is an open-source software framework to simulate the performance of structures subjected to earthquakes (Mazzoni et al., 2007). This paper contributes to the development of this newly added thermo-mechanical analysis capability by integrating the rotational end restraints to the composite beam elements. A part of the 2D unprotected steel frame subassembly is modeled and analyzed using Opensees. The frame consists of a two-floor and two-bay compartment consisting of two composite beams restrained by four columns. One bay is subjected to nonuniform temperature whereas the other bay is kept at ambient temperature to consider the catenary action of the concrete slab from the cold region. The springs with nonlinear moment-rotation curves are defined at the beam end restraints. These spring models take account the rotational allowance of shear connections as well as the decreased stiffness due to beam local buckling. Further, the rebar locations and sizes are varied to observed the effect on the global beam behavior.

1 CARDINGTON BUILDING TEST

In 2003, a large full-scale test on an 8-story steel framed building at Cardington facility (Wald et al., 2006). The goal was to understand the behaviour of beam-to-column and beam-to-beam connections and to quantify the effect of concrete slab on the restrained beams. Fig. 1 illustrates the floor layout of the test. Previously, the subassembly with the single plate connection in the shaded compartment is modeled with three-dimensional solid elements in Abaqus (Selamet and Garlock, 2010). Although the detailed model was very useful to see the local buckling in the connection and the connection failure during the cooling phase, the finite element model required large amount of time to build and run. In this paper, the same secondary beam is represented with a much simpler model to study the effects of connection's rotational capacity and the tensile capacity of the concrete slab during the cooling phase.

(a)   (b)
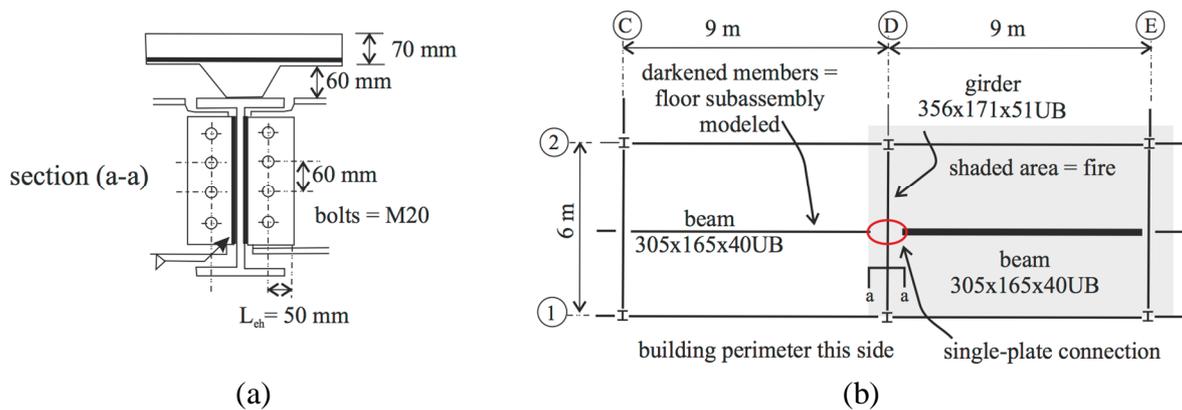
Fig. 1 Details of Cardington building test: (a) single plate connection and (b) the heated building compartment (the modeled beam with thick lines)

In Cardington test, the secondary beam 305x165x40UB is steel with 300 MPa yield strength, the concrete slab is composed of 35 MPa of lightweight concrete (no tensile strength) with A142 anti-crack mesh, which has 320 m^2/m area of steel and 460 MPa of yield strength. The beam is loaded with 21.45 kN/m uniformly distributed load assuming its corresponding tributary area. The structural temperatures are read directly from the thermo-couple readings of Cardington test.

2   THE FINITE ELEMENT MODEL IN OPENSEES

2.1 Description

A recent capability in analyzing the thermo-mechanical problems is added to Opensees by the research team in University of Edinburgh in U.K (Usmani, 2012; Jiang, 2013). In this paper, the realistic scenario of Cardington test is simulated using the structural fire capability of Opensees. For this particular problem, only the secondary (restrained) beam in the heated compartment is investigated. The steel and concrete material properties are adopted from Eurocode 3 (CEN, 2005) by using the *Steel01Thermal* and *Concrete02Thermal* commands. The composite beam is modeled as one section with 8 fibers of concrete slab and 8 fibers of steel beam. The steel mesh is represented as one layer of 8 steel rebars with area of 40 m^2 as illustrated. The effective composite section width is taken from the Steel Construction Manual (AISC, 2005) as 2.25 m, which is one quarter of the total beam length. Only half of the rib area, which runs perpendicular to the beam direction, is added to the concrete slab as shown in Fig. 2.

From the previous research by the authors (Garlock and Selamet, 2010), it was concluded that the cool neighboring compartment (see Fig. 1) provided almost rigid axial constraint to the heated beam. Therefore, the heated beam is axially fully restrained. The *Zerolength Element* command is used to simulate the semi-rigid connection behavior of the single plate shear connection. The single plate connection, as other types of shear connections, has a gap distance that allows limited free rotation (pinned) as seen in Fig. 3. After the gap is closed, the connection behaves as fixed (with high rotational stiffness). Using *UniaxialMaterial ElasticPPGap* command, the realistic behavior of the connection is achieved. The force-deformation character of the *Zerolength Element* is shown in Fig 4. After the gravity load is applied to the beam, the 'Fire Pattern' command is used to apply the structural temperatures at 7 different fiber locations across the composite beam section as shown in Fig. 2. The temperatures are obtained from Cardington test as shown in Fig. 5. The *Corotational* command is used to invoke geometrically nonlinear analysis. A full Newton analysis is done using *algorithm Newton* and *test NormUnbalance* commands.
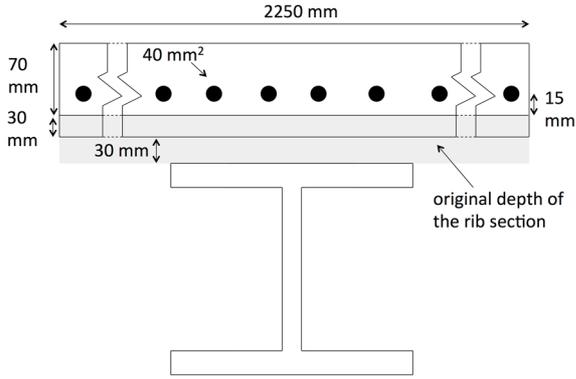
Fig. 2 Composite beam section in Cardington test
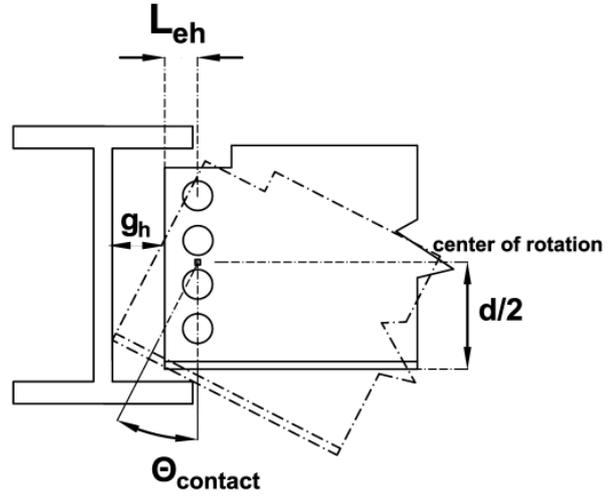
Fig. 3 Composite beam section model in Opensees
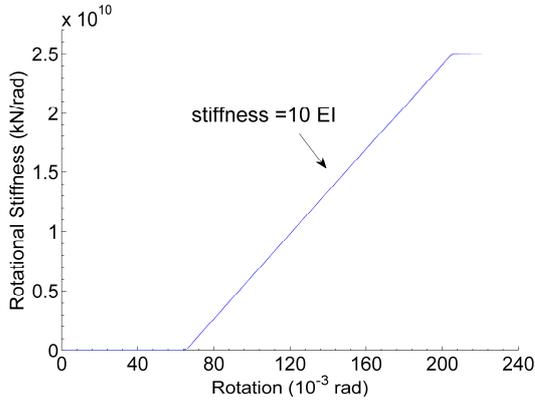
Fig. 4 Semi-rigid connection stiffness of the single-plate connection
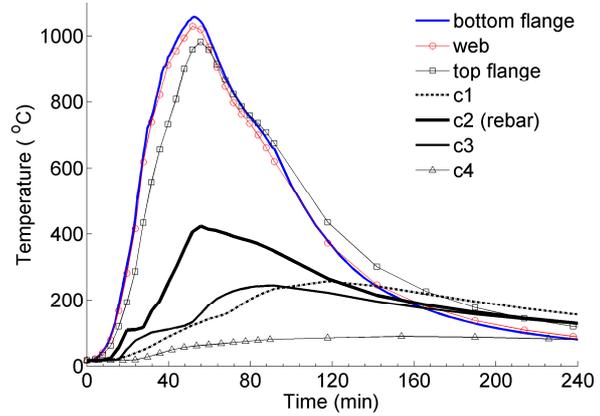
Fig. 5 Fire loading applied to the beam

2.2 Validation

The model in Opensees is compared with the vertical beam midspan deflection obtained from Cardington test. Since the full-scale single plate connection is represented by a 1D rotational spring at the beam end, the spring needs to be calibrated according to the vertical deflection result in the experiment. In addition, an allowable free rotation 65×10^{-3} rad is taken as estimated by *Eq. (1)* (Jaspart, 2003) and illustrated in Fig. 3. Fig. 6 shows that the model with a large rotational stiffness of $10 \ast EI$ (of the steel beam) and the experiment are in close agreement. The heated beam deflects as the stiffness of the steel material decreases. The semi-rigid connection behavior avoids a possible runaway behavior. As the region gets into the cooling phase, the beam contracts and regains some of the deflection but it is significantly limited due to plastic deformations in the beam and in the rebars.

$$\theta_{contact} = \sin^{-1}\left[\frac{L_{eh}+g_h}{\sqrt{L_{eh}^2+(d/2)^2}}\right] - \tan^{-1}\left[\frac{L_{eh}}{d/2}\right] \qquad (1)$$

3   PARAMETRIC STUDY

3.1 Effect of concrete slab

A parametric study is conducted to investigate the effect of the concrete slab and the rebar to the vertical deflection behavior of the composite beam section. As seen in Fig. 6, the bare steel beam experiences runaway behavior and fails during the heating phase of the fire. Further, the composite beam without rebars deflects significantly larger due to the limited tensile capacity of the composite beam. The previously validated composite beam with rebars is in close agreement with the experiment.
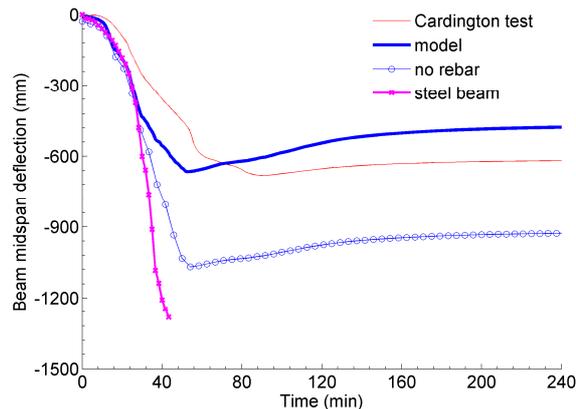
Fig. 6 Vertical deflection of the beam midspan of various parametric studies

3.2 Effect of rebars

Fig. 7a) shows the stress-history in the beam web and in the rebar at the beam end (supports). Independent of the rebar size, it is observed that the rebar's tensile capacity (460MPa) is reached almost immediately after the steel beam yields due to large compression and degrading material properties at elevated temperatures at 300MPa. The stress-strain history of the rebar (not shown) points out that the rebar enters to the unloading (decreasing) stress state at around 2.5% strain during the cooling phase of the fire due to the significant strength regain of the steel beam. Therefore, the stress in the rebar decreases due to large strains after 80 minutes of fire and the regain of the strength is not observed. The increased rebar area increase the tensile stress in the rebar and in the beam web since the beam has deflected much less during the heating with larger rebar (tensile) contribution as clearly seen in Fig. 7b).

Fig. 8a) illustrates the effect of the rebar location on the fire performance of the composite beam. If the rebar is placed further from the beam (closer to the concrete top surface), the rebar carries nearly the same tensile stress as the beam web. As observed in Fig. 8b), the further away the rebar from the beam, it experiences smaller strains. This behavior is expected since the temperatures in the concrete slab are much lower than the temperatures in the steel beam. However, since the yield stress of the rebar is already reached at earlier stages, the strain deformation does not seem to affect the tensile stress development in the beam web during the heating and the cooling phase of the fire.

3.3 Effect of end restraints

The rotational allowance $\theta_{contact}$ is varied from 0 rad to 90×10^{-3} rad (see Fig. 4) with the gap parameter in *UniaxialMaterial ElasticPPGap* command in Opensees. The effect, though insignificant, is seen in early stages of fire in Fig. 9. The rotational spring does not seem to affect the global vertical deflection of the beam midspan mainly because the beam elements near the end supports yield and form a plastic hinge.
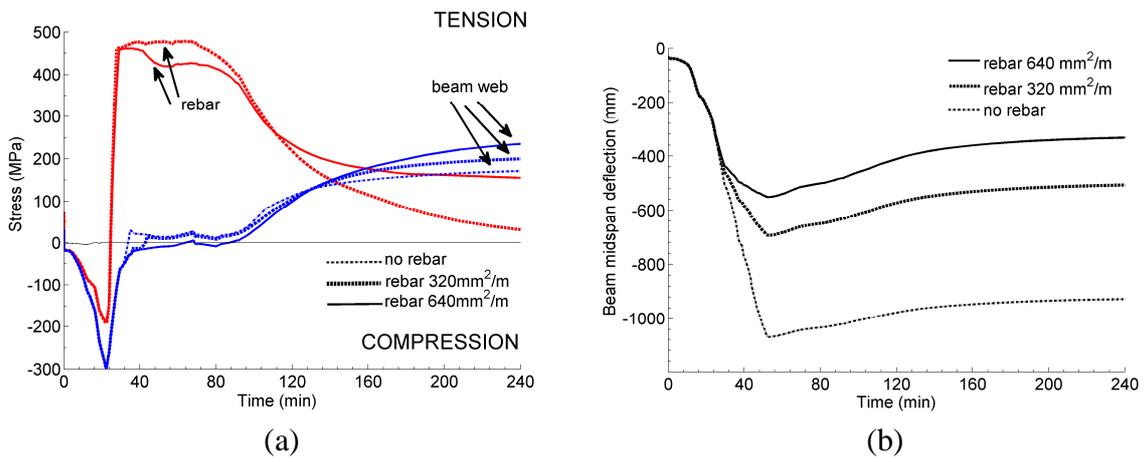
Fig. 7 Stress-strain history of the beam web and the rebar at the beam end with different rebar sizes
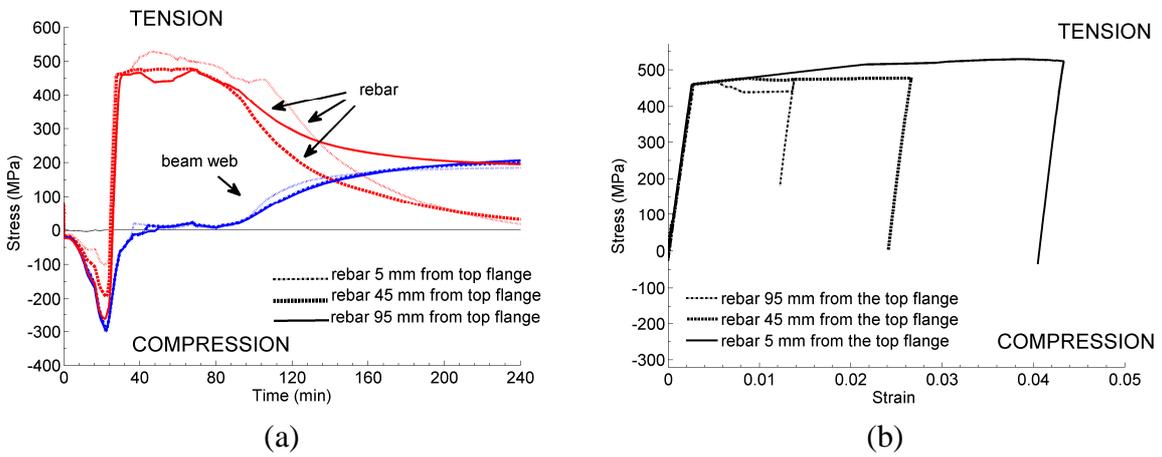
Fig. 8 Stress-strain history of the beam web and the rebar at beam end with different rebar locations
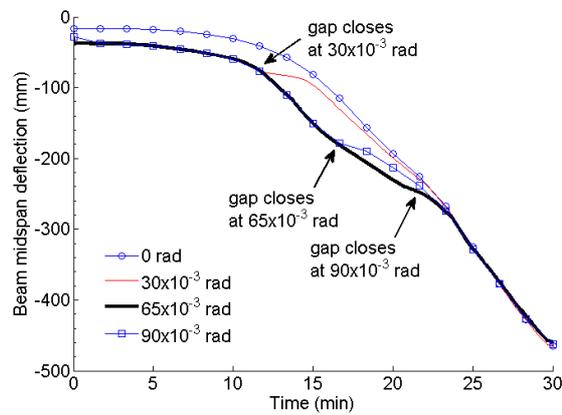
Fig. 9 The vertical beam midspan deflection for various rotational (gap) allowance with the *Zerolength Element*

4   SUMMARY AND ACKNOWLEDGMENT

This paper investigates the behavior of an axially restrained composite beam in Cardington test. A newly developed thermal capability of Opensees is utilized to model and run the analysis. The secondary beam is loaded with large gravity and thermal loading to test its ultimate capacity especially during the cooling phase of the fire. Due to the 1D nature of the beam elements, the full effect of the composite behavior is not observed. It is concluded that Opensees is especially an advantageous tool to create more realistic boundary conditions by using multi-purpose spring elements. However, some convergence problems are reported with using *Steel02Thermal* elements and with *Concrete02Thermal* elements with nonzero tensile capacity. Further, most of the analyses did not converge using *algorithm ModifiedNewton* command.

REFERENCES

AISC, Steel Construction Manual 13th Edition, Chicago, IL, 2005.

CEN, Eurocode 3: Design of Steel Structures Part 1.2: General Rules Structural Fire Design ENV 1993-1-2:2005, Brussels, Belgium, 2005.

Garlock M. and Selamet S., Modeling and Behavior of Steel Plate Connections Subject to Various Fire Scenarios, Journal of Structural Engineering, 136 (7), 897-906, 2010.

Jaspart J.P., European design recommendations for simple joints in steel structures University of Liege, 2003.

Jiang J., Usmani A., Modeling of Steel Frame Structures in Fire using Opensees, Computers and Structures, doi: 10.1016/j.compstruc.2012.07.013, 2013.

Mazzoni S., McKenna F., Scott M. H., Fenves G. L. et al., Opensees Command Language Manual, 2007.

Selamet S. and Garlock M., Robust Fire Design of Single Plate Shear Connections, Engineering Structures, 32 (8), 2367-2378, 2010.

Usmani A., Zhang J., Jiang J., Jiang Y., May I., Using Opensees for Structures in Fire, Journal of Structural Fire Engineering, 3(1), 2012.

Wald F., Simoes da Silva L., Moore D.B., Lennon T., Chladna M., Santiago A., Benes M., Borges L., Experimental Behaviour of a Steel Structure under Natural Fire, Fire Safety Journal, 41 (7), 506-522, 2006.